


Article

Consensus Problem and Formation Control for Heterogeneous Multi-Agent Systems with Switching Topologies

Chunping Wang¹, Jiaqi Wang², Ping Wu² and Jinfeng Gao^{2,*} ¹ Keyi College of Zhejiang Sci-Tech University, Shaoxing 312369, China² School of Information Science and Engineering, Zhejiang Sci-Tech University, Hangzhou 310018, China

* Correspondence: gaojf163@163.com

Abstract: The cooperative control problem of discrete-time multi-agent systems (MASs) is discussed, and bounded uncertain time-delays and directed switching topologies are considered. By applying model transformations and matrix theory, an augmented system method is introduced to handle a heterogeneous time-delay MAS. Then, the consensus problem of the system is turned to the convergence issue of the product of innumerable row stochastic matrices. Sufficient conditions for asymptotic consensus of the system under directed switching topologies are obtained. Moreover, a novel consensus-based formation control strategy is designed to gain sufficient and necessary conditions for the formation control of a second-order differential robot system. Finally, the effectiveness of the obtained results is verified through simulations.

Keywords: cooperative control; discrete-time dynamics; multi-agent systems; uncertain time-delays; switching topologies



Citation: Wang, C.; Wang, J.; Wu, P.; Gao, J. Consensus Problem and Formation Control for Heterogeneous Multi-Agent Systems with Switching Topologies. *Electronics* **2022**, *11*, 2598. <https://doi.org/10.3390/electronics11162598>

Academic Editor: Katarzyna Antosz

Received: 7 August 2022

Accepted: 15 August 2022

Published: 19 August 2022

Publisher's Note: MDPI stays neutral with regard to jurisdictional claims in published maps and institutional affiliations.



Copyright: © 2022 by the authors. Licensee MDPI, Basel, Switzerland. This article is an open access article distributed under the terms and conditions of the Creative Commons Attribution (CC BY) license (<https://creativecommons.org/licenses/by/4.0/>).

1. Introduction

With the popularization of unmanned equipment, the improvement of the automation level and the application of distributed ideas, people have gradually realized that several single agent systems have difficulty in meeting increasingly complex practical needs, such as the cooperative work of multiple handling robots in warehouses, the cooperative equipment of multiple manipulators in factories and multiple unmanned aerial vehicles (UAVs) cluster reconnaissance in military war. Therefore, multi-agent systems (MASs) have emerged as the times require.

MASs originate from the biological cluster phenomenon in nature, such as the formation migration of wild geese and cluster migration of flocks as shown as Figure 1. Then, to meet the needs of engineering, the concept of group behaviors in nature was introduced to the computer field. The goal is to make several single agent systems realize complex intelligence through cooperative control to, thereby, reduce the complexity of system modeling and improve the robustness, reliability and flexibility of the system.

Since the cooperative control of MASs shows the advantages of high autonomy, fault tolerance, coordination, flexibility and scalability, the fields where it may be involved are also wide, such as target positioning [1,2], environmental monitoring [3,4], military exercises [5,6] and resource exploration [7,8]. It can be seen that the application of cooperative control of MASs bring considerable changes to people's daily production and life, even in the national military and medical fields. Up to now, the cooperative control problems of MASs have attracted widespread concern of researchers from the fields of physics, robotics, control engineering, biology, artificial intelligence, etc.



Figure 1. Biological cluster phenomenon in nature. (a) Formation migration of wild geese. (b) Cluster migration of a flock.

Compared with several single agent systems, they can solve more complex practical problems. Therefore, it is necessary to study the cooperative control of MASs. The cooperative control of MASs includes various topics—for example, cooperative output regulation [9–11], consensus [12–14], formation control [15–17] and distributed filtering [18–20].

Formation control and consensus: if the formation control problem is linear (displacement- or bearing-based), then it can be considered as special cases of consensus and matrix-weighted consensus. Distance-based and bearing-only cases are quite different, since the equations governing the systems are nonlinear, and the techniques used for consensus problems cannot be applied directly. These two problems have the most important theoretical and practical significance for the intellectualization of the cooperative control of MASs.

The consensus problem is the primary condition of cooperative control of MASs. It means that agents dynamically adjust and update their behaviors under local cooperation and mutual communication, and all agents finally come to an agreement. The design of distributed consensus control protocol for MASs with general linear dynamics under directed graph is considered in [21]. Li et al. [22] are devoted to consensus problems of second-order MASs under directed topologies. By utilizing local cooperation and distributed control laws, all agents move at a constant speed and finally reach an agreement.

Feng et al. [23] overcame a class of consensus problems of mixed-order MASs using distributed nonlinear consensus control protocols. Komareji et al. [24] discussed the consensus problems in topologically interacting swarms under communication constraints and time-delays. However, there are also some works showing that many MASs (biological and artificial) collectively operate according to a consensus protocol without ever reaching consensus, such as [25].

Formation control problem aims to achieve some complex and global operations by applying some appropriate formation control strategies [26]. Li et al. [27] addressed two kinds of leader-follower formation control problems of second-order autonomous unmanned systems, where the speed of the leader is either constant or time-varying. The hierarchical formation control problems of wheeled mobile robots was investigated using a vector field method in [28]. Liu et al. [29] considered formation tracking control problems of second-order MASs with multiple leaders through sampled data.

However, all the above results represent continuous-time dynamics. In reality, the continuous states of agents are often described and updated by their sampled data, which leads to the formulations of discrete-time dynamics or sampled data. Therefore, the results gained in continuous-time dynamics can not be utilized to settle these issues directly. Under this background, a discrete-time dynamic model was developed in [30]. Chen et al. [31] focused on a new class of cluster consensus problems of discrete-time MASs with a few distinct groups. Cao et al. [32] deliberated on dynamic formation control problems of discrete-time MASs under directed graphs.

Thus far, some important results and methods about switched systems with delays have been established. The consensus of MASs subject to time-varying delayed control inputs and switching topology was considered in [33]. A practical example of a team

of three networked quadrotors is given to illustrate the condition for consensus for a networked system based on linear matrix inequality (LMI) that takes into account the joint effects of time-varying delays and switching network topology.

The time-varying formation problem for nonlinear second-order MASs regarding the existence of switching directed topology and time delay was investigated in [34]. Sufficient conditions for the system to form the desired formation were obtained using the Lyapunov function approach and LMI technique. Nevertheless, research on the cooperative control of discrete-time MASs under multiple constraints was not fully studied. This paper pays close attention to cooperative control of discrete-time MASs with uncertain time-delays and switching topologies.

The motivation of this work is to extend the results in [35,36]. Compared with [35], the research object in Section 3 of this paper becomes more complex and the proposed control algorithm is more accurate. In addition, in Section 4 of this paper, the focus is not consensus of the second-order discrete-time MAS but formation control. Furthermore, the obtained consensus-based formation control strategy in this paper adds the target formation shape and target velocity on the basis of the consensus protocol.

Their functions are shown in Remark 3. In the same way, even though [36] and Section 3 of this paper both studied the consensus problem of heterogeneous MASs, the system model and the corresponding consensus control protocol are different. Both [35,36] are devoted to the study of consensus problem, and sufficient conditions for consensus were obtained. On this basis, this paper also studies the formation control problem.

Furthermore, the necessary and sufficient conditions of formation control are proposed. The results are verified effective by the simulation on Webots platform for Pioneer 3-DX robots. Specifically, our contributions are stated as below. First, different from the Lyapunov function approach mentioned in the literature [37,38], an augmented system method is introduced in this paper. The method can not only deal with a heterogeneous time-delay MAS by applying model transformations and matrix theory but also avoids the difficulty of constructing Lyapunov function to prove the consensus of the system.

Then, the consensus problem of the system is converted to the convergence problem of the product of innumerable row stochastic matrices. Secondly, over the existing results in [30–32], the restrictive conditions for topologies and time-delays are relaxed, arbitrary, bounded uncertain time-delays, and dynamic directed switching topologies that have spanning trees are allowed. Thirdly, a novel consensus-based formation control strategy that only requires local information of neighbors is proposed to gain necessary and sufficient condition for formation control of a second-order differential robot system.

The remaining sections are summarized as below. Section 2 gives some preliminaries. In Section 3, consensus of a heterogeneous time-delay MAS is presented. Formation control of a second-order differential robot system is shown in Section 4. Section 5 is committed to verifying the correctness of the proposed theoretical results via numerical simulations and robot examples. Section 6 offers our conclusions.

Notations: $\omega_n = \{1, \dots, n\}$ is an index set. $i \in \omega_a / \omega_b$ denotes i belongs to ω_a but not to ω_b . R is the real set. I_n represents an n dimensional identity matrix. $\mathbf{1}$ represents a well dimensional column matrix with all ones. \otimes represents the Kronecker product; and $(\cdot)^T$ represents the matrix transpose.

2. Preliminaries

2.1. Graph Theory

A weighted directed graph is represented by $G = (V, E, W)$, where $V = \{1, 2, \dots, n\}$ is a node set, $E \subseteq V \times V$ is a directed edge set and $W = [w_{ij}]$ is a weighted adjacency matrix. In addition, $N_i = \{j \in V, (i, j) \in E\}$ denotes a set of neighbors of node i . A directed edge of G is represented by (i, j) , which means node i points to node j . The indegree of node i is defined as $\deg_{in}(i) = \sum_{j \in N_i} w_{ij}$. The indegree matrix of G is defined as $D = \text{diag}\{\deg_{in}(1), \dots, \deg_{in}(n)\}$.

The Laplacian matrix of G is defined as $L = D - W$. A directed path from node i to node 1 is an ordered sequence of directed edges, which is represented by $(i, i - 1), \dots, (3, 2), (2, 1)$. If there is a node so that there is a directed path from it to each of the remaining nodes, it can be said that the weighted directed graph G has a spanning tree and the node is called root node. The union of some weighted directed graphs $G_{z1}, G_{z2}, \dots, G_{zk}$ with a common node set and a combined directed edge set given by $G_{zj}, j = 1, \dots, k$ is also called a weighted directed graph. The directed switching topologies that have spanning trees means the union of these weighted directed graphs has at least a spanning tree.

2.2. Matrix Theory

Given a matrix $A = [a_{ij}]$, if all elements a_{ij} are not less than zero, then it is a nonnegative matrix. Moreover, if there exists a nonnegative matrix A satisfying $A\mathbf{1} = \mathbf{1}$, then it is a row stochastic matrix. Furthermore, if the row stochastic matrix A satisfying $\lim_{k \rightarrow \infty} A^k = \mathbf{1}f^T$ where f is a column matrix, then it is called indecomposable and aperiodic (SIA) [39].

3. Consensus of Heterogeneous Time-Delay MAS

It should be noted that most studies concentrate on homogeneous systems—that is, all agents have the same-order dynamics. However, the dynamics of the agents may be different because of various restrictions or the common goals with mixed agents in practical systems, such as different spacecraft and robots perform different tasks in the spacecraft and robots formation system.

Thus, it is significant to consider heterogeneous MASs. Compared with the first-order or second-order dynamics MASs, the study of heterogeneous MASs composed of both first-order and second-order dynamics agents seems to be more complicated. Thus, far, there are few results on the consensus of heterogeneous MAS. Therefore, a heterogeneous MAS consists of n agents labeled as $1, 2, \dots, n$ is considered. Agent 1 to agent p ($p < n$) have first-order dynamics, while the remaining agents have second-order dynamics. Then, the discrete-time dynamic model of each agent is presented as:

$$\begin{cases} x_i(k+1) = x_i(k) + u_i(k)T, i \in \omega_p \\ \begin{cases} x_i(k+1) = x_i(k) + v_i(k)T \\ v_i(k+1) = v_i(k) + u_i(k)T, i \in \omega_n/\omega_p \end{cases} \end{cases} \quad (1)$$

where $x_i(k) \in R$, $v_i(k) \in R$ and $u_i(k) \in R$ are, respectively, the position, velocity and control input of agent i at time k . $T > 0$ is the sampling period and $k \geq 0$ indicates the sampling times. For brevity, all kT are replaced by k .

To enable the system (1) to achieve asymptotic consensus with bounded uncertain time-delays and directed switching topologies, a consensus control protocol is designed as:

$$\begin{cases} u_i(k) = p_0 \sum_{j \in N_i} w_{ij}^{r(k)}(k) (x_j(k - \tau_{ij}^{r(k)}(k)) - x_i(k)), i \in \omega_p \\ \begin{cases} u_i(k) = -p_1 v_i(k) + p_2 \sum_{j \in N_i} w_{ij}^{r(k)}(k) (x_j(k - \tau_{ij}^{r(k)}(k)) - x_i(k)) \\ + p_3 \sum_{j \in N_i} w_{ij}^{r(k)}(k) (v_j(k - \tau_{ij}^{r(k)}(k)) - v_i(k)), i \in \omega_n/\omega_p \end{cases} \end{cases} \quad (2)$$

where $p_0 > 0$, $p_1 > 0$, $p_2 > 0$ and $p_3 > 0$ are constant coefficients to be designed. $r(k)$ represents the switching modes of the directed topologies and takes the value from a limited set $S = \{G_1, G_2\}$. $\tau_{ij}^{r(k)}(k)$ represents the uncertain time-delay from agent j to agent i at time k in mode $r(k)$ and satisfies $\tau_{ij}^{r(k)}(k) \leq \tau_{max}$, where τ_{max} is the upper bound of uncertain time-delay depending on the dwell time of the switching topologies. $x_j(k - \tau_{ij}^{r(k)}(k))$ and $v_j(k - \tau_{ij}^{r(k)}(k))$ represent the position and velocity of agent j obtained by agent i at time k

in mode $r(k)$, respectively. $w_{ij}^{r(k)}(k) \geq 0$ is the weighting factor on the directed edge formed by agent i and agent j at time k in mode $r(k)$.

The system (1) realizes asymptotic consensus under the consensus control protocol (2) if Equation (3) holds [37]:

$$\begin{cases} \lim_{k \rightarrow \infty} (x_i(k) - x_j(k)) = 0, \forall i, j \in \omega_n \\ \lim_{k \rightarrow \infty} (v_i(k) - v_j(k)) = 0, \forall i, j \in \omega_n / \omega_p \end{cases} \quad (3)$$

For simplicity, the switching modes of the directed topologies $r(k)$ is selectively ignored. Consider it in the subsequent simulations and make the following changes:

$$\begin{cases} \zeta(k) = [x_1^T(k), \dots, x_p^T(k)]^T \\ \varphi(k) = [x_{p+1}^T(k), v_{p+1}^T(k), \dots, x_n^T(k), v_n^T(k)]^T \end{cases} \quad (4)$$

$$B = \begin{bmatrix} 1 & T \\ 0 & 1 - p_1 T \end{bmatrix} \quad (5)$$

$$C = \begin{bmatrix} 0 & 0 \\ p_2 T & p_3 T \end{bmatrix} \quad (6)$$

$$E = \begin{bmatrix} p_0 T & 0 \\ 0 & p_0 T \end{bmatrix} \quad (7)$$

Then, under the consensus control protocol (2), the system (1) is written as:

$$\begin{cases} \zeta(k+1) = [1 \otimes I_p + (W_{10}(k) - D_1(k)) \otimes E] \zeta(k) + (W_{11}(k) \otimes E) \zeta(k-1) \\ \quad + \dots + (W_{1\tau_{max}}(k) \otimes E) \zeta(k - \tau_{max}), i \in \omega_p \\ \varphi(k+1) = [I_{n-p} \otimes B + (W_{20}(k) - D_2(k)) \otimes C] \varphi(k) + (W_{21}(k) \otimes C) \varphi(k-1) \\ \quad + \dots + (W_{2\tau_{max}}(k) \otimes C) \varphi(k - \tau_{max}), i \in \omega_n / \omega_p \end{cases} \quad (8)$$

where $D_1(k) = \text{diag}(\text{deg}_{in}(1), \dots, \text{deg}_{in}(p))$ and $D_2(k) = \text{diag}(\text{deg}_{in}(p+1), \dots, \text{deg}_{in}(n))$ are the indegree matrices of agent 1 to agent p and agent $(p+1)$ to agent n , respectively. $W_{1m}(k)$ and $W_{2m}(k)$ ($m = 0, 1, \dots, \tau_{max}$) represent the $p \times n$ and $(n-p) \times n$ dimensional weighted adjacency matrices when $\tau_{ij} = m$. According to the definition of a Laplacian matrix, $L_{1m}(k) = D_1(k) - \sum_{m=0}^{\tau_{max}} W_{1m}(k)$ and $L_{2m}(k) = D_2(k) - \sum_{m=0}^{\tau_{max}} W_{2m}(k)$ hold.

To guarantee the asymptotic consensus of the heterogeneous time-delay MAS (8), an augmented system approach is introduced to deal with the system (8) by applying model transformations and matrix theory, while all uncertain time-delays are equal to zero, the coefficient matrices of system (8) still not satisfy the definition of row stochastic matrix. Therefore, the model transformations are used to transform the system (8) into an equivalent system whose coefficient matrices are row stochastic. Finally, the equivalent system is analyzed by the properties of row stochastic matrices and sufficient conditions for asymptotic consensus are obtained.

Let $\hat{v}_i(k) = x_i(k) + H v_i(k)$ and $H = \frac{p_3}{p_2}$. Furthermore, the system (8) is equivalently converted into Equation (9).

$$\begin{cases} \zeta(k+1) = [1 \otimes I_p + (W_{10}(k) - D_1(k)) \otimes E] \zeta(k) + (W_{11}(k) \otimes E) \zeta(k-1) \\ \quad + \dots + (W_{1\tau_{max}}(k) \otimes E) \zeta(k - \tau_{max}), i \in \omega_p \\ \begin{cases} x_i(k+1) = x_i(k) + \frac{\hat{v}_i(k) - x_i(k)}{H} T \\ \hat{v}_i(k+1) = \hat{v}_i(k) + \frac{\hat{v}_i(k) - x_i(k)}{H} (1 - H p_1) T + p_3 \sum_{j=1}^n w_{ij}(k) (\hat{v}_j(k - \tau_{ij}(k)) - \hat{v}_i(k)), i \in \omega_n / \omega_p \end{cases} \end{cases} \quad (9)$$

Denote:

$$\Omega(k) = [x_{p+1}^T(k), \hat{v}_{p+1}^T(k), \dots, x_n^T(k), \hat{v}_n^T(k)]^T \quad (10)$$

$$F = \begin{bmatrix} 1 - \frac{T}{H} & \frac{T}{H} \\ -(1 - Hp_1)\frac{T}{H} & 1 + (1 - Hp_1)\frac{T}{H} \end{bmatrix} \quad (11)$$

$$R = \begin{bmatrix} 0 & 0 \\ 0 & p_3 T \end{bmatrix} \quad (12)$$

Combine Equations (10)–(12), the system (9) is rewritten as:

$$\begin{cases} \zeta(k+1) = [1 \otimes I_p + (W_{10}(k) - D_1(k)) \otimes E] \zeta(k) + (W_{11}(k) \otimes E) \zeta(k-1) \\ \quad + \cdots + (W_{1\tau_{max}}(k) \otimes E) \zeta(k - \tau_{max}), i \in \omega_p \\ \Omega(k+1) = [I_{n-p} \otimes F + (W_{20}(k) - D_2(k)) \otimes R] \Omega(k) + (W_{21}(k) \otimes R) \Omega(k-1) \\ \quad + \cdots + (W_{2\tau_{max}}(k) \otimes R) \Omega(k - \tau_{max}), i \in \omega_n / \omega_p \end{cases} \quad (13)$$

The system (13) is further improved on the basis of system (8), and its coefficient matrices satisfy the definition of row stochastic matrix. However, it still contains uncertain time delays that are not conducive to the analysis of consensus. Therefore, the system (13) needs to be further changed.

Let $\Gamma(k) = [\zeta^T(k), \zeta^T(k-1), \dots, \zeta^T(k - \tau_{max})]^T$ and $\Phi(k) = [\Omega^T(k), \Omega^T(k-1), \dots, \Omega^T(k - \tau_{max})]^T$, an augmented system (14) is described as below:

$$\begin{cases} \Gamma(k+1) = \Psi(k) \Gamma(k) \\ \Phi(k+1) = \Xi(k) \Phi(k) \end{cases} \quad (14)$$

where $\Psi(k)$ and $\Xi(k)$ are given in Equations (15) and (16).

$$\Psi(k) = \begin{bmatrix} 1 \otimes I_p + (W_{10}(k) - D_1(k)) \otimes E & W_{11}(k) \otimes E & \cdots & W_{1\tau_{max}}(k) \otimes E \\ I & 0 & \cdots & 0 \\ 0 & \ddots & \vdots & 0 \\ 0 & \cdots & I & 0 \end{bmatrix} \quad (15)$$

$$\Xi(k) = \begin{bmatrix} I_{n-p} \otimes F + (W_{20}(k) - D_2(k)) \otimes R & W_{21}(k) \otimes R & \cdots & W_{2\tau_{max}}(k) \otimes R \\ I & 0 & \cdots & 0 \\ 0 & \ddots & \vdots & 0 \\ 0 & \cdots & I & 0 \end{bmatrix} \quad (16)$$

Let $\eta(k) = 1 \otimes I_p - D_1(k) \otimes E$ and $\theta(k) = I_{n-p} \otimes F - D_2(k) \otimes R$, Equations (15) and (16) are changed into Equations (17) and (18).

$$\Psi(k) = \begin{bmatrix} \eta(k) + W_{10}(k) \otimes E & W_{11}(k) \otimes E & \cdots & W_{1\tau_{max}}(k) \otimes E \\ I & 0 & \cdots & 0 \\ 0 & \ddots & \vdots & 0 \\ 0 & \cdots & I & 0 \end{bmatrix} \quad (17)$$

$$\Xi(k) = \begin{bmatrix} \theta(k) + W_{20}(k) \otimes R & W_{21}(k) \otimes R & \cdots & W_{2\tau_{max}}(k) \otimes R \\ I & 0 & \cdots & 0 \\ 0 & \ddots & \vdots & 0 \\ 0 & \cdots & I & 0 \end{bmatrix} \quad (18)$$

Let $W_{1m}(k) = [W^{p \times p} \ W^{p \times (n-p)}]$ and $W_{2m}(k) = [W^{(n-p) \times p} \ W^{(n-p) \times (n-p)}]$, then the weighted adjacency matrix W is obtained as follows:

$$W = \begin{bmatrix} W^{p \times p} & W^{p \times (n-p)} \\ W^{(n-p) \times p} & W^{(n-p) \times (n-p)} \end{bmatrix} \quad (19)$$

Since $L(k)\mathbf{1} = 0$, $L_{1m}(k) = D_1(k) - \sum_{m=0}^{\tau_{\max}} W_{1m}(k)$ and $L_{2m}(k) = D_2(k) - \sum_{m=0}^{\tau_{\max}} W_{2m}(k)$, then $\Psi(k)\mathbf{1} = \mathbf{1}$ and $\Xi(k)\mathbf{1} = \mathbf{1}$ hold. In addition, the following two assumptions are need to be made.

Assumption 1. The bounded uncertain time-delays mean that time-delays on each interactive topology can be selected at will, as long as they do not exceed the dwell time of the switching topologies.

$$\tau_{ij}(k) \leq \tau_{\max} \quad (20)$$

Assumption 2. Suppose d_{\max} is the largest principal diagonal element of Laplacian matrix and the following inequalities hold.

$$\begin{cases} p_0 T d_{\max} \leq 1 \\ p_1 H \geq 1 \\ 0 < T \leq H \\ 1 + (1 - p_1 H) \frac{T}{H} \geq p_3 T d_{\max} \end{cases} \quad (21)$$

When Assumptions 1 and 2 are satisfied, all elements of $\Psi(k)$ and $\Xi(k)$ are nonnegative, and satisfy $\Psi(k)\mathbf{1} = \mathbf{1}$ and $\Xi(k)\mathbf{1} = \mathbf{1}$. Therefore, $\Psi(k)$ and $\Xi(k)$ are row stochastic matrices. In addition, for positive integers z_1, z_2, \dots, z_k with $z_k > z_1$, if the union of weighted directed graphs $G_{z_1}, G_{z_2}, \dots, G_{z_k}$ has spanning trees, then $\prod_{k=z_1}^{z_k} \Psi(k)$ and $\prod_{k=z_1}^{z_k} \Xi(k)$ are SIA [40]. In other words, there exists a column matrix f that makes $\prod_{k=z_1}^{z_k} \Psi(k) = \prod_{k=z_1}^{z_k} \Xi(k) = \mathbf{1}f^T$ hold as $z_k \rightarrow \infty$.

Theorem 1. When Assumptions 1 and 2 are satisfied, the heterogeneous time-delay MAS (1) achieves asymptotic consensus under the consensus control protocol (2) if the directed switching topologies have spanning trees.

Proof of Theorem 1. Take into account the augmented system (14). By continuous iteration, Equation (22) is yielded as:

$$\begin{cases} \Gamma(k+1) = \Psi(k)\Psi(k-1) \cdots \Psi(0)\Gamma(0) \\ \Phi(k+1) = \Xi(k)\Xi(k-1) \cdots \Xi(0)\Phi(0) \end{cases} \quad (22)$$

Equation (22) can be simplified as Equation (23):

$$\begin{cases} \Gamma(k+1) = \prod_{m=k}^0 \Psi(m)\Gamma(0) \\ \Phi(k+1) = \prod_{m=k}^0 \Xi(m)\Phi(0) \end{cases} \quad (23)$$

Take the limitation on both sides of Equation (23), Equation (24) is shown as:

$$\begin{cases} \lim_{k \rightarrow \infty} \Gamma(k+1) = \lim_{k \rightarrow \infty} \prod_{m=k}^0 \Psi(m)\Gamma(0) \\ \lim_{k \rightarrow \infty} \Phi(k+1) = \lim_{k \rightarrow \infty} \prod_{m=k}^0 \Xi(m)\Phi(0) \end{cases} \quad (24)$$

As the directed switching topologies have spanning trees, the union of weighted directed graphs $G_{z_1}, G_{z_2}, \dots, G_{z_k}$ for positive integers z_1, z_2, \dots, z_k with $z_k > z_1$ has at least a spanning trees—that is, Equation (25) holds:

$$\begin{cases} \lim_{k \rightarrow \infty} \Gamma(k+1) = \mathbf{1}f^T\Gamma(0) \\ \lim_{k \rightarrow \infty} \Phi(k+1) = \mathbf{1}f^T\Phi(0) \end{cases} \quad (25)$$

According to Equation (25) and all the above analysis, the following Equation (26) holds:

$$\begin{cases} \lim_{k \rightarrow \infty} x_i(k) = \mathbf{1}^T \Gamma(0), i \in \omega_n \\ \lim_{k \rightarrow \infty} v_i(k) = \mathbf{1}^T \Phi(0), i \in \omega_n / \omega_p \end{cases} \quad (26)$$

Then, system (1) achieves asymptotic consensus under the consensus control protocol (2). \square

Corollary 1. *If all uncertain time-delays are equal to zero, the heterogeneous time-delay MAS (1) also realizes asymptotic consensus under the consensus control protocol (2).*

Proof of Corollary 1. While all uncertain time-delays are equal to zero, the situation is seen as an unusual exception of Theorem 1. Furthermore, the remaining analysis is the same as above. Therefore, Corollary 1 holds naturally. \square

Remark 1. *The proposed augmented system method is easier to obtain the sufficient condition for asymptotic consensus of the heterogeneous time-delay MAS (1) under directed switching topologies. Furthermore, the restrictive conditions for topologies and time-delays are relaxed.*

4. Formation Control of Second-Order Differential Robot System

In this part, a second-order differential robot system is shown as:

$$\begin{cases} x_i(k+1) = x_i(k) + v_i(k)T \\ v_i(k+1) = v_i(k) + u_i(k)T, i \in \omega_n \end{cases} \quad (27)$$

where $x_i(k) \in R$, $v_i(k) \in R$, $u_i(k) \in R$ and T are given in Equation (1).

The target formation of the system (27) is given as follows:

$$\xi = [\xi_1, \xi_2, \dots, \xi_n]^T \quad (28)$$

where $\xi_i = [\xi_{ix}, \xi_{iv}]^T$, ξ_{ix} and ξ_{iv} denote, respectively, the target position and target velocity of agent i .

To make the system (27) achieve the target formation shape and run at the target velocity, a novel consensus-based formation control strategy is designed as:

$$\begin{aligned} u_i(k) = & -p_1(v_i(k) - \xi_v) - p_2 \sum_{j \in N_i} w_{ij}^{r(k)}(k)(x_i(k) - x_j(k - \tau_{ij}^{r(k)}(k)) - \xi_{dij}) \\ & - p_3 \sum_{j \in N_i} w_{ij}^{r(k)}(k)(v_i(k) - v_j(k - \tau_{ij}^{r(k)}(k))), i \in \omega_n \end{aligned} \quad (29)$$

The second-order differential robot system (27) achieves the target formation shape and run at the target velocity under the strategy (29) if and only if Equation (30) holds [41].

$$\begin{cases} \lim_{k \rightarrow \infty} (x_i(k) - x_j(k)) = \xi_{dij} \\ \lim_{k \rightarrow \infty} v_i(k) = \lim_{k \rightarrow \infty} v_j(k) = \xi_v, \forall i, j \in \omega_n \end{cases} \quad (30)$$

where $\xi_{dij} = \xi_{ix} - \xi_{jx} = (i - j) * d$, which denotes the relative position of agents i and j measured by sonar sensors. d is the distance between adjacent agents. $\xi_v = \xi_{iv}$ represents target velocity.

Remark 2. *If $\xi_{dij} = 0$, formation control becomes the asymptotic consensus. Furthermore, Equation (30) also becomes $\lim_{k \rightarrow \infty} (\varphi_i(k) - \xi_i) - (\varphi_j(k) - \xi_j) = 0$.*

Similarly, make the following changes:

$$B_1 = \begin{bmatrix} 0 & 0 \\ 0 & p_1 T \end{bmatrix} \quad (31)$$

$$C_1 = \begin{bmatrix} 0 & 0 \\ p_2 T & 0 \end{bmatrix} \quad (32)$$

By substituting the strategy (29) into the system (27) and combining Equations (5), (6), (31) and (32), the system (27) is rewritten as:

$$\begin{aligned} \varphi(k+1) = & [I_n \otimes B - (D_0(k) - W_0(k)) \otimes C_1] \varphi(k) + (W_1(k) \otimes C) \varphi(k-1) + \dots \\ & + (W_{\tau_{\max}}(k) \otimes C) \varphi(k - \tau_{\max}) + (I_n \otimes B_1) \xi - ((D_0(k) - W_0(k)) \otimes C_1) \xi \end{aligned} \quad (33)$$

where $D_0(k) = \text{diag}(\deg(1), \dots, \deg(n))$ is the indegree matrix of agent 1 to agent n and $W_m(k)$ ($m = 0, 1, \dots, \tau_{\max}$) is $n \times n$ dimensional weighted adjacency matrix when $\tau_{ij} = m$.

Further denote:

$$\gamma(k) = \varphi(k) - \xi \quad (34)$$

Then:

$$\varphi(k) = \gamma(k) + \xi \quad (35)$$

Substituting Equation (35) into Equation (33) yields:

$$\begin{aligned} \gamma(k+1) = & [I_n \otimes B - (D_0(k) - W_0(k)) \otimes C] (\gamma(k) + \xi) + (W_1(k) \otimes C) (\gamma(k-1) + \xi) + \dots \\ & + (W_{\tau_{\max}}(k) \otimes C) (\gamma(k - \tau_{\max}) + \xi) + (I_n \otimes B_1) \xi - ((D_0(k) - W_0(k)) \otimes C_1) \xi - \xi \end{aligned} \quad (36)$$

Theorem 2. If and only if $\lim_{k \rightarrow \infty} \gamma_i(k) - \gamma_j(k) = 0$, the second-order differential robot system (27) realizes the target formation shape and run at the target velocity under the strategy (29).

Proof of Theorem 2. (Sufficiency) By substituting Equation (34) into the equation $\lim_{k \rightarrow \infty} \gamma_i(k) - \gamma_j(k) = 0$, $\lim_{k \rightarrow \infty} (\varphi_i(k) - \xi_i) - (\varphi_j(k) - \xi_j) = 0$ holds. According to Equation (30) and Remark 3, it is shown that system (27) realizes the target formation shape and runs at the target velocity.

(Necessity) If the system (27) achieves the target formation shape and run at the target velocity under the strategy (29)—that is, $\lim_{k \rightarrow \infty} (\varphi_i(k) - \xi_i) - (\varphi_j(k) - \xi_j) = 0$ holds. Then, according to Equation (35), $\lim_{k \rightarrow \infty} \gamma_i(k) - \gamma_j(k) = 0$ holds. \square

Remark 3. The benefits of the strategy (29) are that it only requires local information of neighbors instead of centralized control and global shared information to realize the formation control. Furthermore, the target formation shape and target velocity can be adjusted by modifying the parameters d and ξ_v . Therefore, the strategy is suitable for large-scale formation control. Moreover, if the appropriate quantitative information and topology can be found, then consensus algorithm can be guaranteed to converge in a certain time—that is, the strategy can complete the target formation in a certain time.

5. Simulations

To explain the correctness of the obtained results, some numerical simulations and robot examples are presented. Figure 2 shows the switching modes of directed topologies $r(k)$. Let the sampling period $T = 0.2$ s, then the dwell time of switching topologies is $20T$. Therefore, the upper bound of uncertain time-delay is $\tau_{\max} = 4$ s.

5.1. Case 1

The interactive topologies of heterogeneous time-delay MAS (1) with $n = 4$ are given in Figure 3. Suppose agent 1 and agent 2 have first-order dynamics, while the

remaining agents have second-order dynamics. According to the definition of spanning trees, the two interactive topologies have spanning trees. Moreover, since the time-delays on each interactive topology are uncertain but bounded and to satisfy Assumption 1, the time-delays on G_1 and G_2 are arbitrarily selected as 1 and 0.6 s.

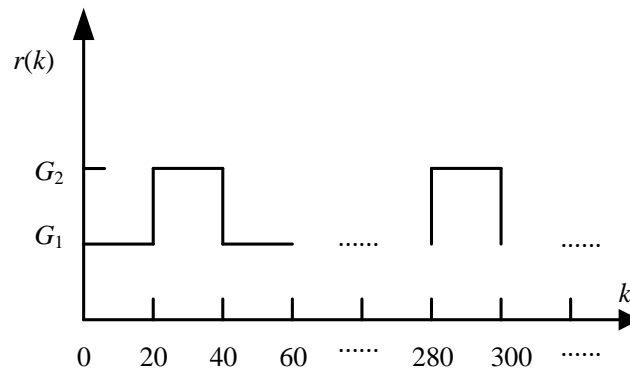


Figure 2. Switching modes of directed topologies $r(k)$.

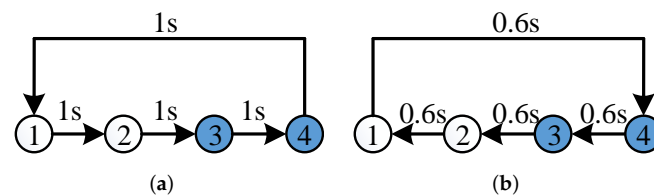


Figure 3. Interactive topologies of heterogeneous time-delay MAS (1). (a) G_1 , (b) G_2 .

If the weighting factor on each edge of the directed topologies is 0.5 and to satisfy the definition that W is a row stochastic matrix [42], then the weighted adjacency matrices of directed graphs G_1 and G_2 are as below:

$$W^{G_1} = \begin{bmatrix} 0.5 & 0 & 0 & 0.5 \\ 0.5 & 0.5 & 0 & 0 \\ 0 & 0.5 & 0.5 & 0 \\ 0 & 0 & 0.5 & 0.5 \end{bmatrix}$$

$$W^{G_2} = \begin{bmatrix} 0.5 & 0.5 & 0 & 0 \\ 0 & 0.5 & 0.5 & 0 \\ 0 & 0 & 0.5 & 0.5 \\ 0.5 & 0 & 0 & 0.5 \end{bmatrix}$$

Since $H = \frac{p_3}{p_2}$, $T = 0.2s$ and $d_{max} = 0.5$, then $0 < p_1 \leq 5$, $0 < p_2 \leq 5p_3$, $p_3^2 \leq 10p_3 + 2p_2 - 2p_1p_3$ and $0 < p_0 \leq 10$ are deduced to satisfy Assumption 2. Therefore, $(p_0, p_1, p_2, p_3) = (1, 1, 1, 2)$ can be chosen. Similar to convergence factors, they directly affect the convergence rate.

Let $x_i(0) = i - 1, i \in I_n$ and $v_i(0) = 0.1 * (i - 1), i \in I_n / I_p$. According to Figure 3 and W , the four agents adjust their state information in real time with the local information of themselves and their neighbors. The ultimate goal is to achieve global state consensus through these local information. By applying the consensus control protocol (2) to the system (1), the position and velocity consensus are shown in Figure 4, which prove the correctness of Theorem 1. Figure 4 shows that the position and velocity trajectories asymptotic convergence about 15s while those asymptotic convergence after 20 s in [43], the convergence rate is about improved by 25% at the cost of increasing the gain parameters and decreasing the number of agents.

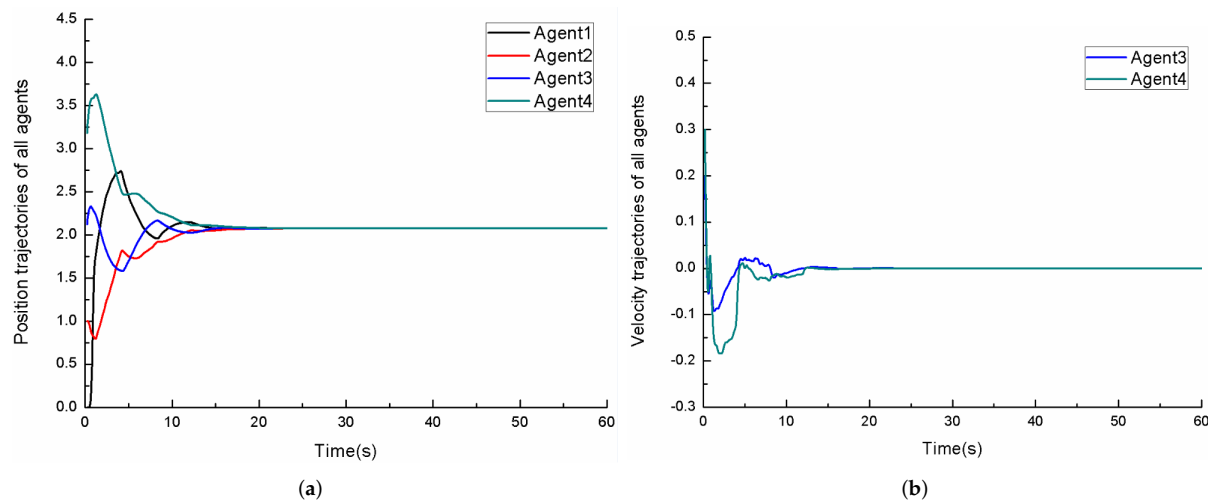


Figure 4. Position and velocity trajectories of heterogeneous time-delay MAS (1). (a) Position trajectories. (b) Velocity trajectories.

5.2. Case 2

The interactive topologies of second-order differential robot system (27) with $n = 4$ are exhibited in Figure 5. Similarly, the time-delays on each interactive topology are uncertain but bounded and to satisfy Assumption 1, the time-delays on G_1 and G_2 are arbitrarily selected as 0.18 and 0.12 s.

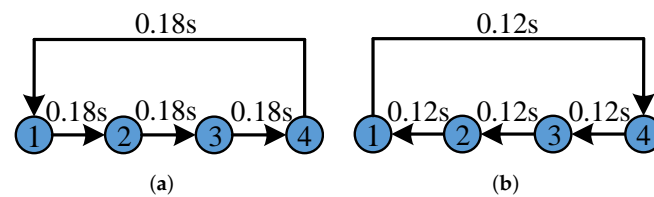


Figure 5. Interactive topologies of second-order differential robot system (27). (a) G_1 , (b) G_2 .

Let $d = 5\text{m}$, $\zeta(v) = 0$ in X direction and $d = 0$, $\zeta(v) = 0.5\text{m/s}$ in Y direction. Furthermore, take $(x_i(0), y_i(0)) = ((6,1), (9,3), (12,6), (20,9))$ and $(v_{xi}(0), v_{yi}(0)) = (0,0)$ for $i \in I_n$. Similar to case 1, the arrows in Figure 5 show the information interaction between agents. Agents achieve cooperative control by continuously adjusting the state information of their neighbors. By applying consensus-based formation control strategy (29) to second-order differential robot system (27), the position and velocity trajectories are shown in Figure 6. Figure 6a,b depict that four agents achieve the target formation shape and run at the target velocity.

Four curves with different colors in Figure 6a represent position trajectories of four agents. From this figure, it can be seen that four agents reach the desired relative positions. Similarly, it can be seen from Figure 6b that the final velocities of the four agents also reach the target velocities. Figure 7 reveals the corresponding position and velocity trajectories when $\tau_{ij}(k) \neq 0$.

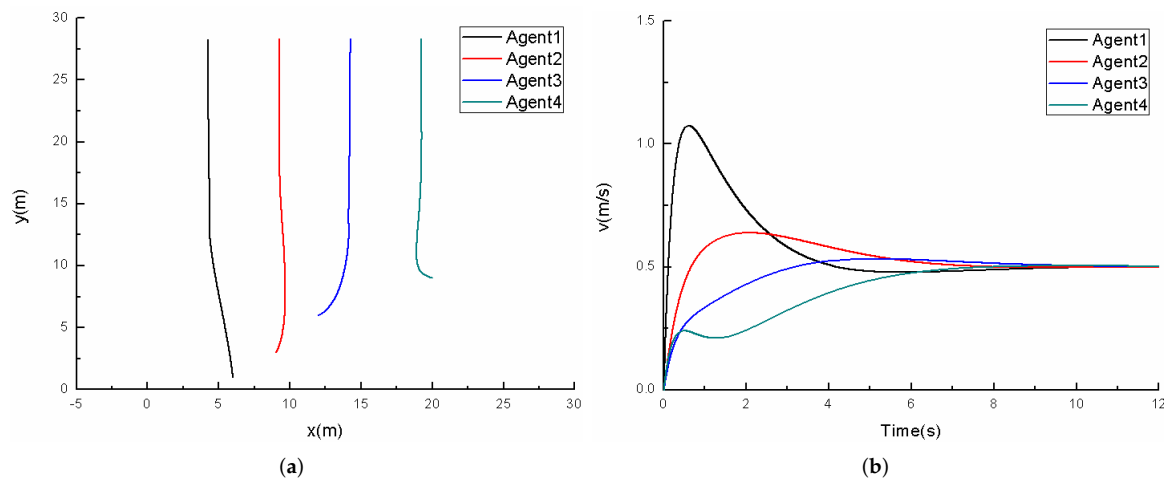


Figure 6. Position and velocity trajectories of second-order differential robot system (27) ($\tau_{ij}(k) = 0$). (a) Position trajectories. (b) Velocity trajectories.

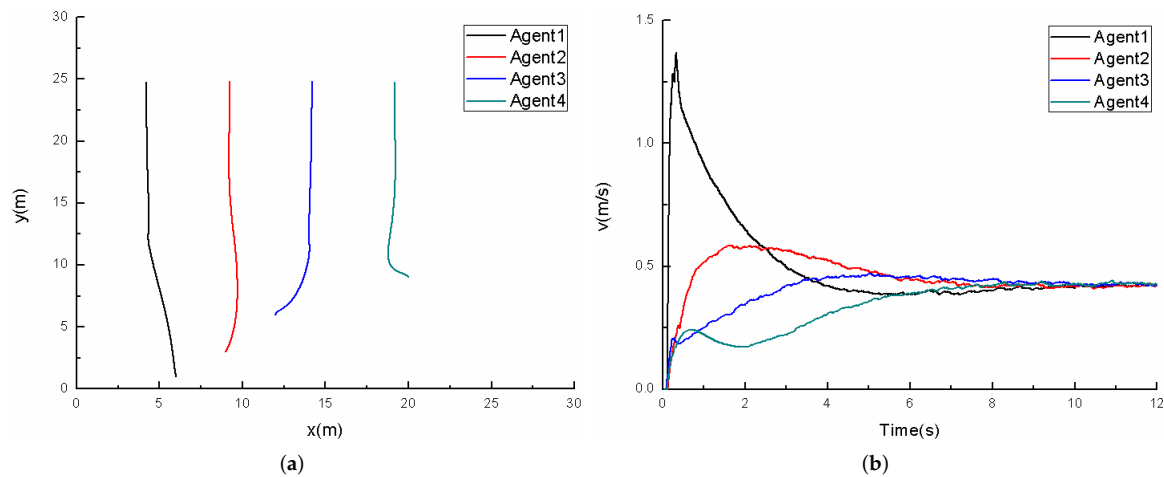


Figure 7. Position and velocity trajectories of second-order differential robot system (27) ($\tau_{ij}(k) \neq 0$). (a) Position trajectories. (b) Velocity trajectories.

Comparing Figures 6 and 7, it is easy to see that the existence of uncertain time delays does have an impact on the convergence rate and overshoot of system (27). However, as long as the uncertain time delays are within the dwell time of switching topologies, the overall convergence characteristics of the system do not change. In addition, Figures 6 and 7 reveal that the position and velocity trajectories are not completely smooth because of the switching topologies.

To further verify the feasibility of formation control of second-order differential robot system (27), four Pioneer 3-DX robots are imported into Webots platform. According to the control requirements, GPS node and Gyro node are added to measure the global position coordinates, velocity and angular velocity. Pioneer 3-DX robots adjust their velocity and direction by means of two wheel differential drive. Furthermore, each wheel is controlled by an independent motor. The dynamic model of second-order differential robot [44] is shown in Figure 8. They mainly rely on the front and rear sonar rings to sense the distance between each other.

There are eight sonars in each sonar ring and 16 sonars in the front and rear. They are eight forward ultrasonic (sonar) sensors and eight optional rear sonars, respectively. Relying on these 16 sonars, the Pioneer 3-DX robot has a 360 degree perception capability. Each sonar has an effective detection range of 30 mm to 5000 mm and a resolution of 1 mm.

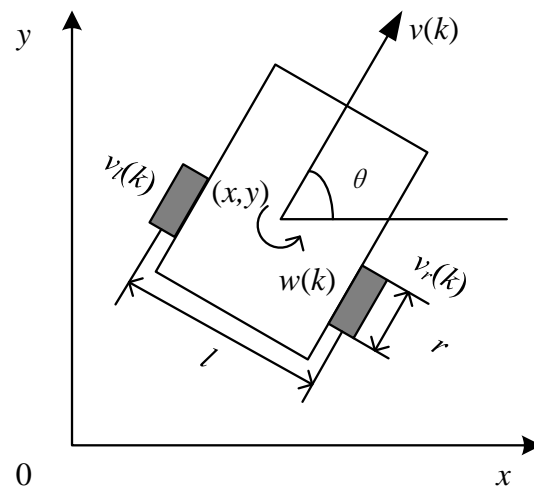


Figure 8. Schematic diagram of second-order differential robot (27).

The $v(k)$ and $w(k)$ denote the velocity and angular velocity, respectively. The $v_l(k)$ and $v_r(k)$ represent the left and right wheel velocities, respectively. The global position coordinates are denoted by (x, y) . l denotes the distance between the left and right wheels, r is the wheel radius [45].

The left and right wheel velocities $v_l(k)$ and $v_r(k)$ are selected as the control variables, and the dynamic model is obtained as shown in (37).

$$\begin{cases} \dot{x} = \frac{r}{2}(v_l(k) + v_r(k))\cos\theta \\ \dot{y} = \frac{r}{2}(v_l(k) + v_r(k))\sin\theta \\ \dot{\theta} = \frac{r}{l}(v_r(k) - v_l(k)) \end{cases} \quad (37)$$

If the robot is regarded as a particle, the velocity $v(k)$ and angular velocity $w(k)$ are selected as the control variables, and the dynamic model is obtained as shown in (38).

$$\begin{cases} \dot{x} = v(k)\cos\theta \\ \dot{y} = v(k)\sin\theta \\ \dot{\theta} = w(k) \end{cases} \quad (38)$$

By synthesizing Equations (37) and (38), eliminating intermediate variables x , y and θ , then the relationships between the left and right wheel velocities and the velocity and angular velocity are obtained as shown in Equation (39). Thus, the dynamic model of the robot with velocity and angular velocity as control variables is obtained as shown in (39).

$$\begin{cases} v_l(k) = \frac{2v(k) - w(k)l}{2r} \\ v_r(k) = \frac{2v(k) + w(k)l}{2r} \end{cases} \quad (39)$$

Let $w(k) = 0$ and initial positions of four robots are taken as $((-2.5, 1.2), (-1, -0.3), (0.5, 0.2)$ and $(1.8, 2.4)$). The strategy (29) is applied to second-order differential robot system (27) to obtain the velocity $v(k)$. According to Equation (39), $v_l(k)$ and $v_r(k)$ are obtained. Finally, the formation achieving processes at $k = 0, 20, 35, 75$ are shown in Figure 9. Clearly, the four Pioneer 3-DX robots form a given target formation shape and run at the target velocity within 15 s.



Figure 9. The formation shape of four robots at $k = 0, 20, 35, 75$. (a) Formation shape ($k = 0$). (b) Formation shape ($k = 20$). (c) Formation shape ($k = 35$). (d) Formation shape ($k = 75$).

6. Conclusions

The cooperative control problem of discrete-time MASs with bounded uncertain time-delays and directed switching topologies is considered. By applying model transformations and matrix theory, an augmented system approach is introduced to make the consensus of the heterogeneous time-delay MASs transform into the convergence issue of the product of innumerable row stochastic matrices. Moreover, a novel consensus-based formation control strategy is devised so that the second-order differential robot system realizes target formation. Furthermore, the effectiveness of the obtained results is verified through some simulations.

Author Contributions: Methodology, writing-original draft, C.W.; Simulation, validation, J.W.; Writing—review & editing, P.W.; Investigation, J.G. All authors have read and agreed to the published version of the manuscript.

Funding: This research was funded by the National Natural Science Foundation of China under Grant 62073296 and Zhejiang Province Public Welfare Technology Application Research Project under Grant LGF19F030004 and Keyi College of Zhejiang Sci-Tech University Academy of Science Project under Grant KY2022006.

Conflicts of Interest: The authors declare no conflict of interest.

References

- Franchi, A.; Stegagno, P.; Di Rocco, M.; Oriolo, G. Distributed Target Localization and Encirclement with a Multi-Robot System. *IFAC Proc. Vol.* **2010**, *43*, 151–156. [\[CrossRef\]](#)
- Bourne, J.R.; Goodell, M.N.; He, X.; Steiner, J.A.; Leang, K.K. Decentralized multi-agent information-theoretic control for target estimation and localization: Finding gas leaks. *Int. J. Robot. Res.* **2020**, *39*, 1525–1548. [\[CrossRef\]](#)
- Sabol, C.; Burns, R.; Mclaughlin, C.A. Satellite Formation Flying Design and Evolution. *J. Spacecr. Rocket.* **2001**, *38*, 270–278. [\[CrossRef\]](#)
- Srivastava, I.; Bhat, S.; Singh, A.R. Fault diagnosis, service restoration, and data loss mitigation through multi-agent system in a smart power distribution grid. *Energy Sources Part A Recovery Util. Environ. Eff.* **2020**, 1–26. [\[CrossRef\]](#)
- Franch, A.; Secchi, C.; Ryll, M.; Bulthoff, H.H.; Giordano, P.R. Shared Control Balancing Autonomy and Human Assistance with a Group of Quadrotor UAVs. *IEEE Robot. Autom. Mag.* **2012**, *19*, 57–68. [\[CrossRef\]](#)
- Li, X.; Dong, Z.M.; He, X. Platform-level Distributed Warfare Model-based on Multi-Agent System Framework. *Def. Sci. J.* **2012**, *62*, 180–186. [\[CrossRef\]](#)
- Boudoudouh, S.; Ouassaid, M.; Maaroufi, M. Multi agent system in a distributed energy management of a multi sources system with a hybrid storage. In Proceedings of the third IEEE International Renewable and Sustainable Energy Conference, Marrakech, Morocco, 10–13 October 2015; pp. 1–6.
- Kovalenko, I.; Ryashentseva, D.; Vogel-Heuser, B.; Tilbury, D.; Barton, K. Dynamic Resource Task Negotiation to Enable Product Agent Exploration in Multi-Agent Manufacturing Systems. *IEEE Robot. Autom. Lett.* **2019**, *4*, 2854–2861. [\[CrossRef\]](#)
- Ma, Q.; Xu, S.Y.; Lewis, F.L.; Zhang, B.; Zou, Y. Cooperative Output Regulation of Singular Heterogeneous Multi-Agent Systems. *IEEE Trans. Cybern.* **2017**, *46*, 1471–1475. [\[CrossRef\]](#)
- Wang, S.M.; Huang, J. Cooperative Output Regulation of Singular Multi-Agent Systems Under Switching Network by Standard Reduction. *IEEE Trans. Circuits Syst. I Regul. Pap.* **2018**, *65*, 1377–1385. [\[CrossRef\]](#)
- Su, Y.F.; Huang, J. Cooperative Global Adaptive Output Regulation for Nonlinear Uncertain Multi-agent Systems with IISS Inverse Dynamics. *Asian J. Control.* **2015**, *17*, 14–22. [\[CrossRef\]](#)
- Liu, L.; Shan, J.J. Event-triggered consensus of nonlinear multi-agent systems with stochastic switching topology. *J. Frankl. Inst.* **2017**, *354*, 5350–5373. [\[CrossRef\]](#)

13. Chen, Y.; Lü, J.H.; Lin, Z.L. Consensus of Discrete-Time Multi-Agent Systems with Transmission Nonlinearity. *Automatica* **2013**, *49*, 1768–1775. [\[CrossRef\]](#)
14. Chen, Y.; Dong, H.R.; Lu, J.H.; Sun, X.; Liu, K. Robust Consensus of Nonlinear Multi-Agent Systems with Switching Topology and Bounded Noises. *IEEE Trans. Cybern.* **2017**, *46*, 1276–1285. [\[CrossRef\]](#)
15. Wang, H.F.; Mei, Y.; Xie, G.M.; Shi, H. Event-triggered circle formation control of multi-agent systems. In Proceedings of the 33rd Chinese Control Conference, Nanjing, China, 28–30 July 2014.
16. Zhang, T.Y.; Liu, G.P. Design of formation control architecture based on leader-following approach. In Proceedings of the 2015 IEEE International Conference on Mechatronics and Automation, Beijing, China, 2–5 August 2015.
17. Xue, D.; Yao, J.; Wang, J.; Guo, Y.; Han, X. Formation control of multi-agent systems with stochastic switching topology and time-varying communication delays. *IET Control Theory Appl.* **2013**, *7*, 1689–1698. [\[CrossRef\]](#)
18. Yu, H.Y.; Liu, Y.S.; Wang, W. Distributed sparse signal estimation in sensor networks using H_∞ -consensus filtering. *IEEE/CAA J. Autom. Sin.* **2014**, *1*, 149–154.
19. Battistelli, G.; Chisci, L.G.; Forti, N.; Pelosi, G.; Selleri, S. Distributed Finite-Element Kalman Filter for Field Estimation. *IEEE Trans. Autom. Control* **2017**, *62*, 3309–3322. [\[CrossRef\]](#)
20. Roshany-Yamchi, S.; Cychowski, M.; Negenborn, R.R.; De Schutter, B.; Delaney, K.; Connell, J. Kalman Filter-Based Distributed Predictive Control of Large-Scale Multi-Rate Systems: Application to Power Networks. *IEEE Trans. Control Syst. Technol.* **2013**, *21*, 27–39. [\[CrossRef\]](#)
21. Li, Z.K.; Wen, G.H.; Duan, Z.S.; Ren, W. Designing Fully Distributed Consensus Protocols for Linear Multi-Agent Systems with Directed Graphs. *IEEE Trans. Autom. Control* **2015**, *60*, 1152–1157. [\[CrossRef\]](#)
22. Li, X.; Gao, K.; Lin, P.; Mo, L. A further result on consensus problems of second-order multi-agent systems with directed graphs, a moving mode and multiple delays. *ISA Trans.* **2017**, *71*, 21–24. [\[CrossRef\]](#)
23. Feng, Y.Z.; Tu, X.M. Consensus analysis for a class of mixed-order multi-agent systems with nonlinear consensus protocols. *Trans. Inst. Meas. Control* **2014**, *37*, 147–153. [\[CrossRef\]](#)
24. Komareji, M.; Shang, Y.; Bouffanais, R. Consensus in topologically interacting swarms under communication constraints and time-delays. *Nonlinear Dyn.* **2018**, *93*, 1287–1300. [\[CrossRef\]](#)
25. Horsevad, N.; Mateo, D.; Kooij, R.E.; Barrat, A.; Bouffanais, R. Transition from simple to complex contagion in collective decision-making. *Nat. Commun.* **2022**, *13*, 1–10. [\[CrossRef\]](#) [\[PubMed\]](#)
26. Chen, Y.Y.; Wang, Z.Z.; Zhang, Y.; Liu, C.L.; Wang, Q. A geometric extension design for spherical formation tracking control of second-order agents in unknown spatiotemporal flowfields. *Nonlinear Dyn.* **2017**, *88*, 1173–1186. [\[CrossRef\]](#)
27. Li, Y.Z.; Wu, Y.Q.; He, S.H. Network-based leader-following formation control of second-order autonomous unmanned systems. *J. Frankl. Inst.* **2020**, *358*, 757–775. [\[CrossRef\]](#)
28. Kwon, J.W.; Chwa, D. Hierarchical Formation Control Based on a Vector Field Method for Wheeled Mobile Robots. *IEEE Trans. Robot.* **2012**, *28*, 1335–1345. [\[CrossRef\]](#)
29. Liu, C.Y.; Wu, X.Q.; Mao, B. Formation Tracking of Second-Order Multi-Agent Systems With Multiple Leaders Based on Sampled Data. *IEEE Trans. Circuits Syst. II Express Briefs* **2020**, *68*, 331–335. [\[CrossRef\]](#)
30. Tanner, H.G.; Christodoulakis, D.K. State synchronization in local-interaction networks is robust with respect to time delays. In Proceedings of the 44th IEEE Conference on Decision and Control, Seville, Spain, 15 October 2015.
31. Chen, Y.; Lü, J.H.; Han, F.L.; Yu, X. On the cluster consensus of discrete-time multi-agent systems. *Syst. Control Lett.* **2011**, *60*, 517–523. [\[CrossRef\]](#)
32. Cao, K.; Li, X.X.; Xie, L.H. Preview-Based Discrete-Time Dynamic Formation Control Over Directed Networks via Matrix-Valued Laplacian. *IEEE Trans. Cybern.* **2020**, *50*, 1251–1263. [\[CrossRef\]](#)
33. Savino, H.J.; dos Santos, C.R.P.; Souza, F.O.; Pimenta, L.C.; De Oliveira, M.; Palhares, R.M. Conditions for Consensus of Multi-Agent Systems With Time-Delays and Uncertain Switching Topology. *IEEE Trans. Ind. Electron.* **2016**, *63*, 1258–1267. [\[CrossRef\]](#)
34. Li, F.H.; Han, L.; Dong, X.W.; Ren, Z. Time-Varying Formation for Second Order Nonlinear Multi-agent System with Switching Topology and Time Delay. In Proceedings of 2019 Chinese Automation Congress, Hangzhou, China, 22–24 December 2019; pp. 2979–2984.
35. Lin, P.; Jia, Y.M. Consensus of second-order discrete-time multi-agent systems with nonuniform time-delays and dynamically changing topologies. *Automatica* **2009**, *45*, 2154–2158. [\[CrossRef\]](#)
36. Liu, C.L.; Liu, F. Stationary consensus of heterogeneous multi-agent systems with bounded communication delays. *Automatica* **2011**, *47*, 2130–2133. [\[CrossRef\]](#)
37. Zheng, Y.S.; Zhu, Y.R.; Wang, L. Consensus of heterogeneous multi-agent systems. *IET Control Theory Appl.* **2011**, *5*, 1881–1888. [\[CrossRef\]](#)
38. Wang, B.B.; Sun, Y.G. Consensus Analysis of Heterogeneous Multi-Agent Systems with Time-Varying Delay. *Entropy* **2015**, *17*, 3631–3644. [\[CrossRef\]](#)
39. Wolfowitz, J. Products of indecomposable, aperiodic, stochastic matrices. *Proc. Am. Math. Soc.* **1963**, *14*, 733. [\[CrossRef\]](#)
40. Xiao, F.; Wang, L. State Consensus for Multi-Agent Systems with Switching Topologies and Time-Varying Delays. *Int. J. Control* **2006**, *79*, 1277–1284. [\[CrossRef\]](#)

41. Hua, Y.Z.; Dong, X.W.; Li, Q.D.; Ren, Z. Distributed Fault-Tolerant Time-Varying Formation Control for Second-Order Multi-Agent Systems With Actuator Failures and Directed Topologies. *IEEE Trans. Circuits Syst. II Express Briefs* **2018**, *65*, 774–778. [[CrossRef](#)]
42. Ren, W.; Beard, R.W. *Distributed Consensus in Multi-Vehicle Cooperative Control: Theory and Applications*; Springer: Berlin/Heidelberg, Germany, 2008.
43. Liu, K.; Ji, Z.J.; Xie, G.M.; Wang, L. Consensus for heterogeneous multi-agent systems under fixed and switching topologies. *J. Frankl. Inst.* **2015**, *352*, 3670–3683. [[CrossRef](#)]
44. Kim, J.; Kim, B.K. Cornering Trajectory Planning Avoiding Slip for Differential-Wheeled Mobile Robots. *IEEE Trans. Ind. Electron.* **2020**, *67*, 6698–6708. [[CrossRef](#)]
45. Filipescu, A.; Stancu, A.I.; Filipescu, S.; Stamatescu, G. On-line parameter estimation in sliding-mode control of Pioneer 3-DX wheeled mobile robot. In Proceedings of the Seventh Conference on Seventh WSEAS International Conference on Systems Theory and Scientific Computation, Athens, Greece, 24–26 August 2017.